IEEE Photonics Journal
An IEEE Photonics Society Publication

Open Access

# Eight-Channel Optical Add-Drop Multiplexer With Cascaded Parent-Sub Microring Resonators

Volume 7, Number 4, August 2015

Xian Xiao
Xiangdong Li
Xue Feng
Kaiyu Cui
Fang Liu
Yidong Huang, Member, IEEE

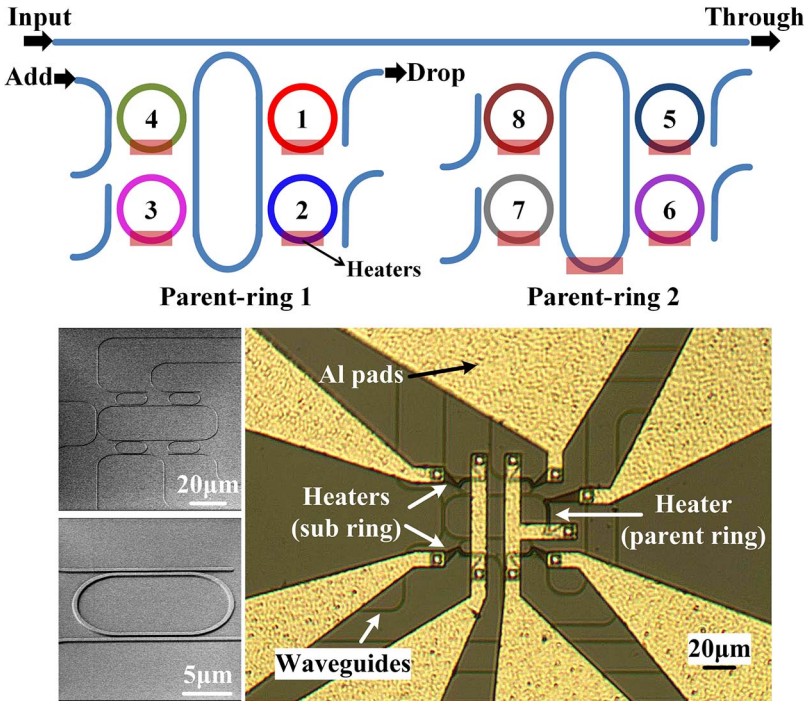


DOI: 10.1109/JPHOT.2015.2464103
1943-0655 © 2015 IEEE

# Eight-Channel Optical Add-Drop Multiplexer With Cascaded Parent-Sub Microring Resonators

**Xian Xiao, Xiangdong Li, Xue Feng, Kaiyu Cui, Fang Liu, and Yidong Huang, *Member, IEEE***

Department of Electronic Engineering, Tsinghua National Laboratory for Information Science and Technology, Tsinghua University, Beijing 100084, China

*DOI: 10.1109/JPHOT.2015.2464103*


Manuscript received June 5, 2015; revised July 25, 2015; accepted July 30, 2015. Date of publication August 3, 2015; date of current version August 12, 2015. This work was supported in part by the National Basic Research Program of China under Grant 2011CBA00608 and Grant 2011CBA00303 and in part by the National Natural Science Foundation of China under Grant 61307068 and Grant 61321004. Corresponding author: X. Feng (e-mail: x-feng@tsinghua.edu.cn).

**Abstract:** An eight-channel integrated optical add-drop multiplexer with cascaded parent-sub microring resonators is experimentally demonstrated on a silicon-on-insulator (SOI) substrate. Through thermal tuning, each channel can be independently switched between the adding and dropping states. The measured thermal tuning efficiency is 0.15 nm/mW. Typically, all eight channels can be multiplexed and demultiplexed with a 2.6-dB drop loss, a 0.36-nm bandwidth ($>$ 40 GHz), and a $-$20-dB channel crosstalk. Moreover, the scheme to increase the number of operating channels is also discussed.

**Index Terms:** Optical add-drop multiplexer (OADM), microring, optical interconnects.

## 1. Introduction

Silicon photonics makes optical interconnection a potential solution for high-performance chip-scale communication owing to the high data transmission rate, low power consumption, and compatibility with standard complementary metal-oxide semiconductor (CMOS) processes [1], [2]. To effectively increase transmission capacity, wavelength division multiplexing (WDM) is necessary [3]. In an on-chip WDM transmission system, integrated optical add-drop multiplexer (OADM) is a fundamental device that allows adding and dropping WDM channels. Until now, several approaches have been demonstrated to implement integrated OADM including echelle grating [4], arrayed waveguide grating [5], cascaded Mach–Zehnder interferometer [6], and microring [7]. Among them, microring approach exhibits the smallest footprint as well as the add/drop filter structure is particularly suitable for integrated OADM. For microring based OADM, however, it is challenging to achieve large free spectral range (FSR), box-like passband, and uniform channel spacing at the same time with fewer heaters and low fabrication requirement. In our previous work [8], we presented a four-channel OADM with parent-sub ring resonators structure that combines all of benefits mentioned above. However, more operating channels and higher transmission rate is still required to meet the demand of modern computing system.

In this paper, we experimentally demonstrated an eight-channel optical add-drop multiplexer with cascaded parent-sub microring resonators. The device is fabricated on silicon-on-insulator

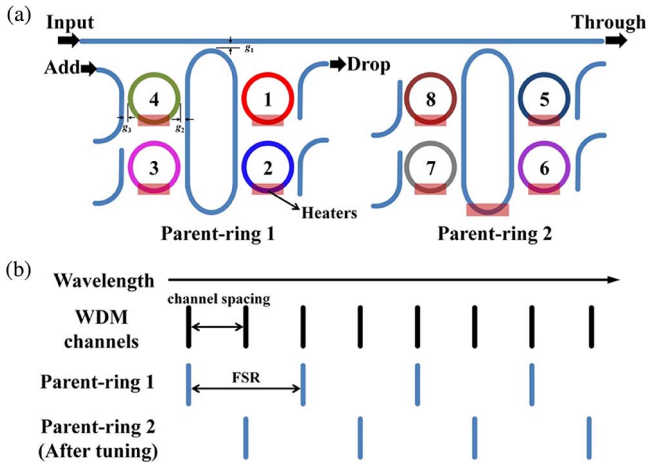


Fig. 1. (a) Layout of eight-channel OADM with two cascaded units of parent-sub microring resonators. (b) Schematic of the wavelength relation between the WDM channels and the parent-ring resonances.

(SOI) substrate with CMOS-compatible technology. By thermally tuning the second parent-ring and all eight sub-rings, the channel spacing can be kept uniform and each channel can be switched between the states of adding and dropping. Comparing with the simple structure of cascaded microring array [7], our approach exhibits advantages of second-order filter response and uniform FSR as discussed in our previous work [8]. The measured results show that, all 8 channels can be de-multiplexed with drop loss of 2.6 dB, bandwidth of 0.36 nm ($>$ 40 GHz), and channel crosstalk of $-20$ dB. On the other hand, one channel can be multiplexed with adding loss of 2.2 dB, bandwidth of 0.35 nm, and through-port suppression ratio of 18 dB. Moreover, two schemes to further increase the operating channels are also discussed.

## 2. Principle, Design and Fabrication

Fig. 1(a) shows the layout of our proposed 8-channel OADM. Two cascaded parent-rings with nearly identical perimeters are coupled to a bus waveguide and each of them is surrounded by four sub-rings with smaller perimeter. The detailed design of each parent-sub ring unit can be found in our previous work [9]. Here, with proper thermal tuning, the resonances of parent-ring 2 would be located between two adjacent resonances of parent-ring 1 as shown in Fig. 1(b). Then, the resonant wavelengths of the two parent-rings are considered as the center wavelength of incident WDM channels. For instance, the odd channels (channel 1, 3, 5, 7) are resonances of parent-ring 1, and the even ones (channel 2, 4, 6, 8) are those of parent-ring 2. In consequence, the WDM channel spacing equals to half FSR of each parent-ring. After the parent-rings are well prepared, the resonances of 8 sub-rings could be independently switched to align/misalign to one of the 8 WDM channels so that the corresponding WDM signals could be controlled to output from the drop-port/through-port and the function of adding/dropping is achieved. Obviously, the operation wavelength of sub-rings 1–4 correspond to the four WDM channels of parent-ring 1 as well as sub-rings 5–8 correspond to those of parent-ring 2.

In this work, the wavelengths of the WDM signals are assumed to be around 1550 nm with 1.6 nm channel spacing. All waveguides in the fabricated sample are silicon rib waveguides with width of 500 nm, height of 220 nm, and a slab layer of 60 nm. The estimated group refractive index is 4.29 for fundamental transverse electric (TE) mode. Thus, the perimeters of parent-rings are determined with $L_1 = 174.83$ $\mu$m for parent-ring 1 and $L_2 = 175.11$ $\mu$m for parent-ring 2. The little difference is to make the resonance wavelengths of the parent-rings staggered. For the same reason, the perimeters of sub-rings are set as shown in Table 1. Considering the fabrication error and ambient temperature variation, a heater is added on parent-ring 2 to tune the resonance. As discussed in our previous work [8], according to the operating bandwidth, flatness of

TABLE 1

Perimeters of sub-rings

| *Sub-ring* | 1 | 2 | 3 | 4 | 5 | 6 | 7 | 8 |
|---|---|---|---|---|---|---|---|---|
| *Perimeter (μm)* | 46.54 | 46.66 | 46.79 | 46.91 | 46.54 | 46.66 | 46.79 | 46.91 |

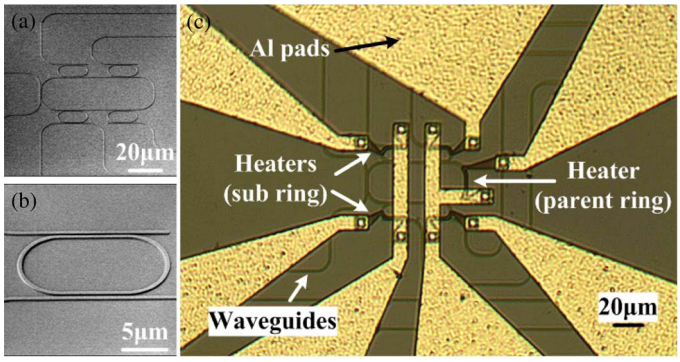


Fig. 2. (a) and (b) Defect review scanning electron microscope (DRSEM) images of microring resonators without $SiO_2$ cladding layer. (c) Microscope image of the fabricated parent-ring 2 and circumambient sub-rings with micro-heaters on each of them.

passband and channel crosstalk, the gap distance between bus waveguide and parent-rings $(g_1)$, parent-rings and sub-rings $(g_2)$ as well as sub-rings and waveguides $(g_3)$ are carefully designed as $g_1 = 200$ nm, $g_2 = 330$ nm, and $g_3 = 200$ nm, respectively.

The device is fabricated on an SOI wafer through the photonics prototyping service at the Institute of Microelectronics (IME) in Singapore. The thickness of the top silicon layer and buried oxide layer is 220 nm and 2 $\mu$m, respectively. A 248 nm deep UV lithography is used to define the pattern. Then the waveguides are etched with inductively coupled plasma reactive ion etch (ICP-RIE) [see Fig. 2(a) and (b)]. After depositing $SiO_2$ cladding on top of the waveguides, TiN heaters are formed on the cladding over the sub-rings and parent-ring 2 as thermally tuning structure. The heaters are 2 $\mu$m wide and connect to the Al pads [see Fig. 2(c)].

## 3. Measurements and Results

The fabricated sample is characterized by measuring the spectra of all output ports. A tunable laser serves as a light source while the lightwave is rotated by a polarization controller to excite fundamental TE mode in the silicon rib waveguide. Single-mode lensed tapered fibers are mounted on a computer-controlled alignment stage to couple light in and out of the device. The spectra are obtained by recording the output power with wavelength scanning step of 0.05 nm.

Fig. 3(a) shows the measured spectra of all output ports without thermal tuning. The 8 dips in the through-port response (black line) represent the resonances of parent-rings (1542.8 nm, 1546.05 nm, 1549.2 nm, and 1552.45 nm for parent-ring 1 and 1544.8 nm, 1548.05 nm, 1551.2 nm, and 1554.5 nm for parent-ring 2). Thus, the FSR for parent-rings is 3.2 nm and the channel spacing is 1.6 nm. We assume that the resonances of parent-ring 1 automatically calibrate the positions of odd channels and the even channels are obtained by tuning the parent-ring 2. The FSR of sub-rings is measured to be 12 nm. Due to Vernier effect, the FSR of our proposed OADM would be 48 nm.

With proper thermal tuning of all 8 sub-rings and parent-ring 2, the function of dropping WDM signals is achieved. Here, some probes are connected with the electrodes to input electrical signals for thermal tuning. Since the number of probes is limited, the 8 channels are measured separately. As shown in Fig. 2(b), the black lines represent the through-port spectra, while the

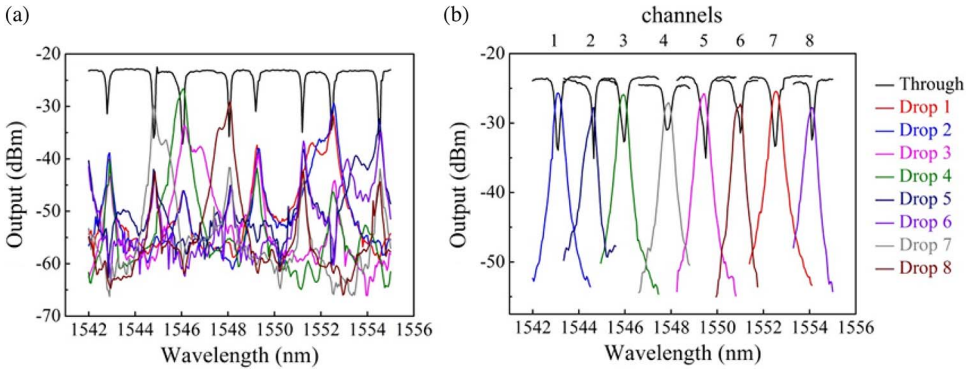


Fig. 3. Measured output power spectra without thermal tuning (a) and with tuning so that the resonances of sub-rings match the eight channels (b).

TABLE 2

Power consumptions and measured parameters for each channel under dropping state

| Channel No. | 1 | 2 | 3 | 4 | 5 | 6 | 7 | 8 |
|---|---|---|---|---|---|---|---|---|
| *Wavelength (nm)* | 1543.1 | 1544.65 | 1545.95 | 1547.8 | 1549.5 | 1551 | 1552.5 | 1554.1 |
| *Parent-ring* | 1 | 2 | 1 | 2 | 1 | 2 | 1 | 2 |
| *Sub-ring (Drop-port)* | 2 | 5 | 4 | 7 | 3 | 8 | 1 | 6 |
| *Power for sub-rings (mW)* | 22.5 | 18.9 | 1.0 | 17.1 | 18.3 | 26.5 | 6.7 | 3.7 |
| *Power for parent-rings (mW)* | 0 | 86.3 | 0 | 85.6 | 0 | 86.5 | 0 | 86.1 |
| *3-dB bandwidth (nm)* | 0.35 | 0.3 | 0.35 | 0.4 | 0.35 | 0.4 | 0.4 | 0.35 |
| *Drop loss (dB)* | 2.1 | 3.5 | 2.4 | 2.5 | 2.4 | 3.3 | 1.9 | 2.5 |
| *Shape factor* | 0.31 | 0.21 | 0.29 | 0.29 | 0.28 | 0.4 | 0.36 | 0.29 |

colored lines represent those of drop-port. The power consumptions and other measured parameters are listed in Table 2. To align the resonances of parent-ring 2 to even channels, the required wavelength shift may be from 0 nm to FSR of parent-rings. In our sample, the value is 3 nm and the corresponding tuning power is about 86 mW. The wavelengths of channels 1–8 are from 1543.1 nm to 1554.1 nm as shown in Table 2. Due to fabrication error, there is resonance divergence to the original design for each sub-ring so that the resonance of sub-ring should be tuned. In order to minimize the average power consumption, the resonance of each sub-ring is thermally tuned to wavelength of the nearest operating channel. Specifically, the sub-rings around parent-ring 1 are set to channel number of 7, 1, 5, 3 (odd channels), while those around parent-ring 2 are set to channel number of 2, 8, 4, 6 (even channels) as shown in Table 2. The averaged 3-dB bandwidth for eight channels is 0.36 nm ($>$ 40 GHz), the averaged drop loss is 2.6 dB, and the averaged shape factors (1 dB–10 dB bandwidth ratio) is 0.3. The variety of parameters between different channels is mainly caused by different alignment accuracy.

Next, the adding function of sub-ring 4 is tested. Fig. 4(a) and (b) show the output power spectra of dropping and adding state. Both of them are measured with the same tuning power (1.0 mW) to make sure the resonance wavelength of sub-ring 4 is aligned to channel 3. For adding state, the WDM signal inputs from sub-ring 4, then goes through the parent-ring 1 and outputs from through-port of bus waveguide with loss of 2.2 dB. It could be seen that, both the passbands in Fig. 4 are nearly flat. However, the through-port extinction of adding state is 18.2 dB which is larger than that of dropping state (9.2 dB). That is because the wavelength scanning step is not small enough.

Furthermore, two sub-rings are simultaneously tuned to dropping state. Fig. 5(a) shows the output spectra of through-port, drop-port 2 and 4 when sub-rings 2 and 4 are aligned to

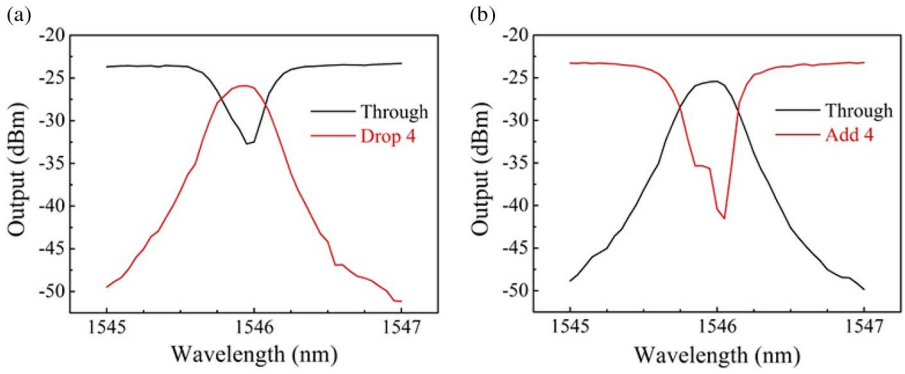


Fig. 4. Output spectra of (a) through-port and drop-port 4 when signal is dropped from sub-ring 4 and (b) through-port and add-port 4 when signal is added from sub-ring 4.

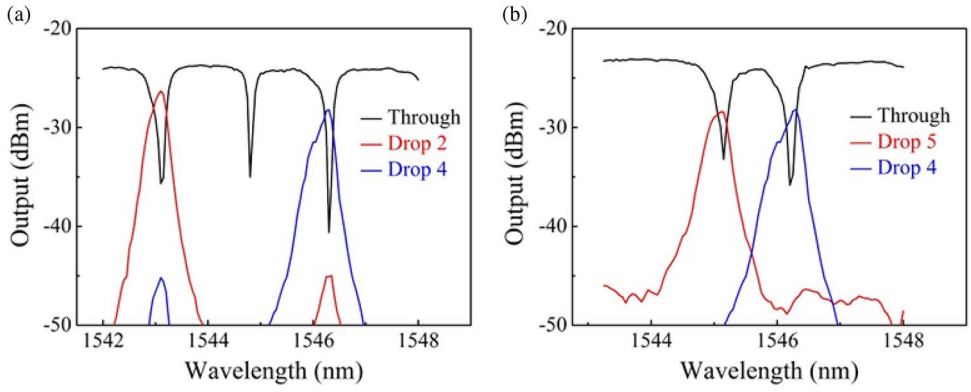


Fig. 5. Output spectra of: (a) channels 1 and 3 are dropped from sub-rings 2 and 4 and (b) channels 2 and 3 are dropped from sub-rings 5 and 4.

channels 1 and 3 with the corresponding tuning powers of 23.3 mW and 2.3 mW, respectively. It could be observed that the channel crosstalk between sub-rings which belong to the same parent-ring is about $-20$ dB. Moreover, the channels 2 and 3 are tuned to be dropped from sub-rings 5 and 4 [see Fig. 5(b)] with the corresponding tuning powers of 24.8 mW and 2.3 mW, respectively. It could be seen that there is nearly no crosstalk between adjacent channels since the adjacent WDM channels are isolated by different parent-rings.

The electrical properties of the heaters are also measured. The resistances of all eight heaters of sub-rings are $155 \pm 5\ \Omega$. The black line in Fig. 6(a) shows that the resonance wavelength shift and the applied electric power exhibit a linear relationship with a slope of 0.15 nm/mW. A slight resonance shift in the surrounding parent-ring is also observed (0.01 nm/mW, red line in Fig. 6(a)), which is probably due to the thermal crosstalk. However, there is no resonance shift observed in the other parent-ring since the distance is relatively far and the thermal crosstalk could be ignored. For the heater of parent-ring 2, the resistance is $213 \pm 4\ \Omega$, and the tuning efficiency is 0.04 nm/mW with a crosstalk of 0.01 nm/mW for sub-ring 6 and 7 [see Fig. 6(b)].

## 4. Discussion

In this work, two cascaded units of parent-sub rings are employed to achieve an 8-channel OADM. According to experimental results, the thermal tuning power consumption is higher than that in our previous work [8], as shown in Table 2. The power consumption is mainly determined by two factors. The first one is the resonance misalignment between the parent-ring and sub-ring due to fabrication errors, and the maximum power consumption would be the value that

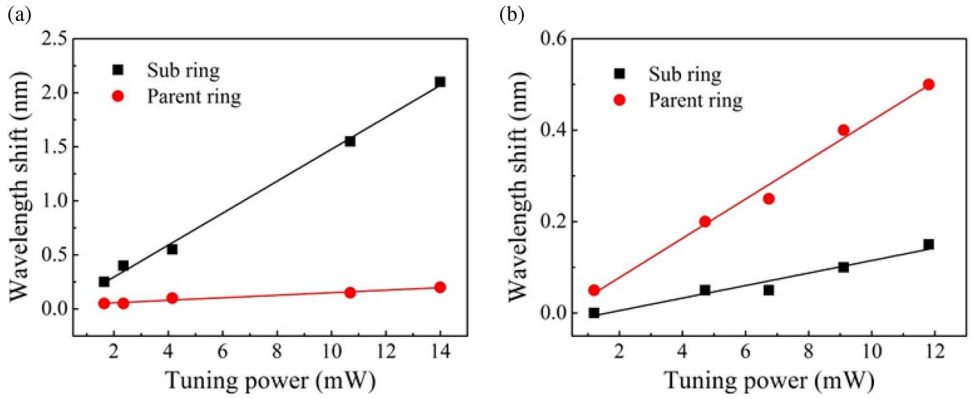


Fig. 6. Thermal tuning power versus corresponding resonance wavelength shift of parent and sub-rings for (a) heaters of sub-rings and (b) heater of parent-ring 2.

could shift the resonance wavelength of a sub-ring to the FSR of the parent-ring. For our measured sample, the value is ~21.3 mW. For a practical device, this value could be reduced with high-precision fabrication technology.

The other factor that influences the power consumption is the tuning efficiency of heaters. In this work, we have moved the heaters of sub-rings away from parent-rings so that the wavelength shift caused by thermal crosstalk is much lower than our previous work [8]. However, as a parasitical disadvantage, the heater efficiency is reduced since the heaters cover less part of all rings. As a result, the power consumption in this work is relatively higher than that of our previous work [8]. In order to enhance the heater efficiency and minimize the thermal crosstalk at the same time, two solutions have been demonstrated including free-standing microring structure [10] and thermal isolation trenches around heaters [11]. Among them, we tend to utilize thermal isolation trenches for practical devices after considering mechanical hardness.

Actually, to scale up the number of operating channels, there is another option that is to increase the perimeter of parent-ring and set more sub-rings surrounded. Next, we will briefly discuss such two approaches. First, larger ring perimeter will lead to larger footprint, as well as more thermal crosstalk to parent-ring. For instance, if the channel number is increased from 4 to 16 with only one parent-ring and 16 sub-rings, the perimeter of parent-ring will increase from 175 $\mu$m to 1015 $\mu$m. Moreover, 16 sub-rings means 16 heaters with 16 crosstalk signals, which is adverse to the stability of the device. On the contrary, with cascaded structure shown in this work, although four cascaded units are required, the perimeter of parent-ring could be also ~175 $\mu$m, and the thermal signals of each sub-ring only affect their subordinate parent-ring. Thus, we believe that the cascading scheme is more preferable for increasing the number of operating channels.

## 5. Conclusion

In this paper, we experimentally demonstrated an 8-channel optical add-drop multiplexer with cascaded parent-sub microring resonators on SOI substrate. Typically, all eight channels can be multiplexed and de-multiplexed independently with 2.6 dB drop loss, 0.36 nm bandwidth ($>$ 40 GHz), and $-$20 dB channel crosstalk. Moreover, the cascading scheme is proved to be more practicable to increase the channel number.

## Acknowledgment

The authors would like to thank H. Yan and Z. Huang for their valuable discussions and helpful comments. The authors also thank the Institute of Microelectronics, Singapore, for device fabrication.

## References


[1] T. Barwicz *et al.,* "Silicon photonics for compact, energy-efficient interconnects," *J. Opt. Netw.*, vol. 6, no. 1, pp. 63–73, Jan. 2006.

[2] A. V. Krishnamoorthy *et al.,* "Computing microsystems based on silicon photonic interconnects," *Proc. IEEE*, vol. 97, no. 7, pp. 1337–1361, Jul. 2009.

[3] X. Zheng *et al.,* "A tunable 1 $\times$ 4 silicon CMOS photonic wavelength multiplexer/demultiplexer for dense optical interconnects," *Opt. Exp.*, vol. 18, no. 5, pp. 5151–5160, Mar. 2010.

[4] F. Horst, W. M. J. Green, B. J. Offrein, and Y. A. Vlasov, "Silicon-on-insulator echelle grating WDM demultiplexers with two stigmatic points," *IEEE Photon. Technol. Lett.*, vol. 21, no. 23, pp. 1743–1745, Dec. 2009.

[5] T. Fukazawa, F. Ohno, and T. Baba, "Very compact arrayed-waveguide-grating demultiplexer using Si photonic wire waveguides," *Jpn. J. Appl. Phys.*, vol. 43, no. 5B, pp. L673–L675, May 2004.

[6] D. W. Kim *et al.,* "Silicon-on-insulator eight-channel optical multiplexer based on a cascade of asymmetric Mach–Zehnder interferometers," *Opt. Lett.*, vol. 33, no. 5, pp. 530–532, Mar. 2008.

[7] M. Geng *et al.,* "Four-channel reconfigurable optical add-drop multiplexer based on photonic wire waveguide," *Opt. Exp.*, vol. 17, no. 7, pp. 5502–5516, Mar. 2009.

[8] H. Yan *et al.,* "Compact optical add-drop multiplexers with parent-sub ring resonators on SOI substrates," *IEEE Photon. Technol. Lett.*, vol. 25, no. 15, pp. 1462–1465, Aug. 2013.

[9] H. Yan, X. Feng, D. Zhang, and Y. Huang, "Integrated optical add-drop multiplexer based on a compact parent-sub microring-resonator structure," *Opt. Commun.*, vol. 289, pp. 53–59, Feb. 2013.

[10] P. Dong *et al.,* "1 $\times$ 4 reconfigurable demultiplexing filter based on free-standing silicon racetrack resonators," *Opt. Exp.*, vol. 18, no. 24, pp. 24 504–24 509, Nov. 2010.

[11] P. Dong *et al.* "Low power and compact reconfigurable multiplexing devices based on silicon microring resonators," *Opt. Exp.*, vol. 18, no. 10, pp. 9852–9858, May 2010.